

Cite this: *Dalton Trans.*, 2013, **42**, 13425

Synthesis, structural characterization, VHPO mimicking peroxidative bromination and DNA nuclease activity of oxovanadium(v) complexes†

Swarup Patra, Suparna Chatterjee, Tapan Kr. Si and Kalyan K. Mukherjea*

The two novel oxovanadium(v) complexes [VO(PyDC)(BHA)] (**1**) [PyDC = pyridine-2,6-dicarboxylate, BHA = benzohydroxamate] and [VO(PyDC)(BPHA)] (**2**) [BPHA = benzophenyl hydroxamate] were synthesized by successive addition of a methanolic solution of H₂PyDC and the corresponding hydroxamic acid ligand to the aqueous solution of ammonium metavanadate (NH₄VO₃). The hydroxamic acid ligands were characterized by elemental analysis, IR, UV-vis and NMR studies whereas the complexes were characterized by IR, UV-vis, CHN, molar conductance, magnetic moment, mass and NMR spectroscopic methods. The structures of the complexes were determined by single crystal X-ray crystallography. The structures of both complexes reveal that vanadium(v) has distorted octahedral geometry. The bromoperoxidase activities of these complexes have been demonstrated through the activation of C–H bonds of phenol, *o*-cresol and *p*-cresol. The catalytic products have been characterized by GC-MS analysis which shows that good conversions have been achieved. So far as the catalytic efficiency of the complexes are concerned complex **2** is found to be superior to complex **1**. Both the complexes were tested for DNA nuclease activity with pUC19 plasmid DNA. The results show that both of them exhibited nuclease activity against pUC19 circular plasmid DNA. The complexes produced both nicked coils and linear forms. In this case also it is observed that complex **2** shows better nuclease activity than complex **1**.

Received 16th May 2013,
Accepted 9th July 2013

DOI: 10.1039/c3dt51291f

www.rsc.org/dalton

Introduction

The coordination chemistry of vanadium with multidentate ligands is receiving special attention because of the potential therapeutic^{1–6} and catalytic^{7–10} application of vanadium complexes. Modelling the structure and monitoring the activity of various vanadium containing biomimetic and biomimicking molecules have also influenced research on vanadium chemistry. Examples of interest in this context are the naturally occurring vanadium dependent haloperoxidases (VHPO).^{11,12} Vanadium dependent haloperoxidase enzymes isolated from different sources such as *Ascophyllum nodosum* (brown algae),¹³ *Corallina officinalis* (red algae),¹⁴ and *Curvularia inaequalis* (fungi)¹⁵ have been structurally characterized and

they exhibit a high degree of amino acid homology in their active centres leading to almost identical active site structures.¹⁶ Reactions involving the oxidative bromination of organic substrates catalysed by vanadium complexes in the presence of halide under physiological conditions have been considered as model reactions for ‘VHPO’^{17–21} enzymes. This is an important route for the biosynthesis of many useful natural halogenated organic compounds.²² Moreover, the oxovanadium(v) complexes are also used in homogeneous catalysis of oxygen transfer in the field of oxidation reactions of various organic compounds (hydrocarbons, alcohols,^{23–29} organic sulfide^{30,31} etc.). The synthesis of transition metal complexes capable of cleaving DNA at specific sites has been an area of considerable current interest because it plays a major role in genomic research, photodynamic therapy of cancer,^{32,33} and the development of new tools for nanotechnology.^{34,35} Many oxovanadium(v) complexes have been shown to have the potentiality of nitrogen fixation,³⁶ insulin mimetism^{37–40} and antitumor⁴¹ and antiamebic⁴² activities, while many other such complexes have been known to be the initiators in the photo-cleavage of DNA.^{43,44} Therefore, reactivity of oxovanadium(v) complexes is receiving renewed attention in the fields of both bromination of organic compounds *via* bromide oxidation and the development of DNA cleavage reagents. However, reports in relation to

Department of Chemistry, Jadavpur University, Kolkata-700032, India.

E-mail: k_mukherjea@yahoo.com; Fax: +91-33-2414-6584; Tel: +91-9831129321

†Electronic supplementary information (ESI) available: The figures of gas chromatograph (Fig. S1–S6), GC-Mass spectra (Fig. S7–S14), absorption spectra of the complexes in presence and absence of increasing amounts of DNA (Fig. S15 and S16), hydrogen bonding (Tables S1 and S2) and bond distances and bond angles of the above two complexes (Table S3) are available as ESI. CCDC 870238 and 870239 for complexes **1** and **2** respectively. For ESI and crystallographic data in CIF or other electronic format see DOI: 10.1039/c3dt51291f

the interaction of vanadium complexes^{45–48} with DNA are rather scant. On the other hand, the hydroxamic acid derivatives are good analytical reagents and have important biological implications due to their siderophoric role.¹⁶ Hence, the foregoing facts prompted us to make an attempt to design and develop the vanadium based hydroxamate complexes in order to employ them in mimicking enzymatic functions. As a result of such an attempt, we could develop two new enzyme mimicking oxovanadium complexes, *viz.* [VO(PyDC)(BHA)] (**1**) and [VO(PyDC)(BPHA)] (**2**).

Results and discussion

Characterisation of the complexes

IR and UV-vis spectroscopic characterization of the complex.

The IR spectra of pyridine-2,6-dicarboxylic acid [H₂PyDC] show a strong absorption band in the region 3067–2535 cm⁻¹ due to the O–H stretching mode^{49,50} of the COOH group. The other two stretching vibrations of the H₂PyDC ligand at 1705⁵⁰ and 1573 cm⁻¹ assignable to $\nu_{\text{asym}(\text{COO}^-)}$ and $\nu_{\text{sym}(\text{COO}^-)}$, respectively, are shifted to 1674 and 1557 cm⁻¹ in complex **1** and 1700 and 1537 cm⁻¹ in complex **2**. This downward shift in $\nu_{(\text{COO}^-)}$ vibrations is suggestive of the involvement of carboxylate O-atom in chelating with the metal ion in both the complexes. The $\nu_{\text{V=O}}$ vibrations in complexes **1** and **2** appear at 989 and 987 cm⁻¹ respectively.^{24,51} In uncoordinated benzohydroxamic acid [BHAH] and benzophenylhydroxamic acid [BPHAH] the $\nu_{(\text{C=O})}$, $\nu_{(\text{N-O})}$ and $\nu_{(\text{C-N})}$ stretching frequencies appear at 1608, 920, 1487 cm⁻¹ and 1623, 925, 1491 cm⁻¹⁵² respectively. The shifting of the $\nu_{(\text{CO})}$ vibration to lower energy indicates the coordination of the carbonyl oxygen to the vanadium(v) center in both the cases. The minimal shifting of $\nu_{(\text{C-N})}$ vibrations of BHAH and BPHAH ligands to 1485 cm⁻¹ in complex **1** and 1488 cm⁻¹ in complex **2** indicates a marginal change in C–N bond order after coordination. The stretching frequencies of the $\nu_{(\text{N-O})}$ after complexation appear at 914 and 918 cm⁻¹ in complexes **1** and **2** respectively.

No d–d transition bands are expected for either of the complexes as there are no d electrons. Complexes **1** and **2** exhibit ligand [P_{II} (O⁻²)] to metal [V(d_{xy})] charge transfer (LMCT) transition at 268 and 269 nm respectively. The other bands that appeared at 222 and 225 nm in complexes **1** and **2** respectively are due to intraligand transitions.^{53–55}

¹H NMR spectra of the complex. ¹H NMR spectrometry lends strong support in the elucidation of the structure of the compound. The signals recorded at 8.3–8.2 ppm in the ligand spectrum are due to the presence of three aromatic protons in H₂PyDC. The presence of multiple proton signals in the range 8.7–8.3 ppm in complex **1** and one triplet at 8.5 ppm (*J* = 7.7 Hz) as well as one doublet at 8.3 ppm (*J* = 7.6 Hz) in complex **2** indicates the coordination of the H₂PyDC to the metal centre in both the complexes. The signal observed at 9.1 ppm in the BPHAH ligand has disappeared in complex **2**, as a result of the deprotonation of the –OH group during coordination. The multiple proton signals appearing at

7.7–7.4 ppm in BHAH and at 7.4–7.2 ppm in BPHAH due to the presence of the aromatic protons are shifted to 7.8–7.5 ppm in complex **1** and 7.6–7.2 ppm in complex **2**. This clearly indicates that the ligands BHAH and BPHAH are involved in coordination with the metal in complexes **1** and **2** respectively.

Molecular structure of complexes 1 and 2. The coordination geometry around the metal center in complexes **1** (Fig. 2) and **2** (Fig. 4) can be described as distorted octahedral with the oxo oxygen (O1 in complexes **1** and **2**) and carboxyl oxygen (O7 in complexes **1** and **2**) atoms occupying the apical sites. The corresponding basal planes are defined by three donor atoms (O3, O4, N2 in complexes **1** and **2**) of the tridentate pyridine-2,6-dicarboxylate ligand (PyDC²⁻) and one oxygen atom (O6 in complexes **1** and **2**) from the hydroxamate ligand (BHA in **1** and BPHA in **2**). The axial V=O bond distances V1–O1 in complex **1** and complex **2** are 1.5804(16) Å⁵³ and 1.5770(17) Å⁵⁶ respectively. The vanadium atom is displaced from the basal plane towards the oxo ligand by 0.241(1) Å and 0.237 Å in complexes **1** and **2** respectively. As a result, the V–O bond distance [V1–O7 in **1** and **2**] *trans* to the oxo ligand is elongated to 2.1594(13) Å and 2.1471(15) Å in complexes **1** and **2** respectively as compared to the corresponding equatorial bond lengths (Table 1). The equatorial V1–N2 bond distance in **1** is 2.0422(14) Å which is nearly the same as in **2** [2.0548(17) Å]. The unit cells of the crystals of complexes **1** and **2** contain eight and six asymmetric [VO(PyDC)(BHA)] and [VO(PyDC)(BPHA)] units respectively. The packing pattern in complex **1** (Fig. 3) shows that a zigzag one dimensional infinite molecular

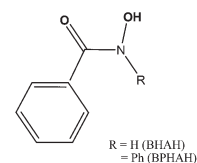


Fig. 1 Structural representation of benzohydroxamic acid (BHAH) and *N*-benzophenylhydroxamic acid (BPHAH).

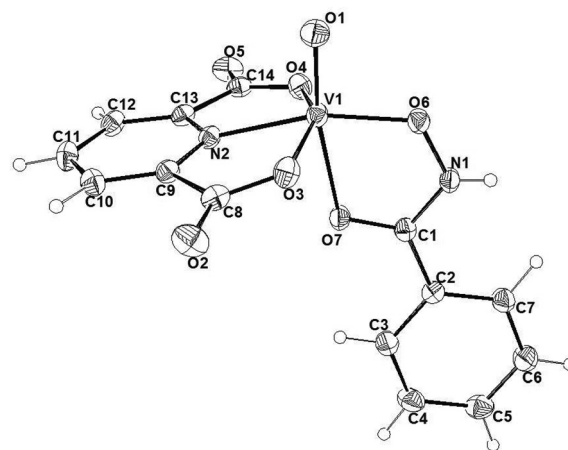
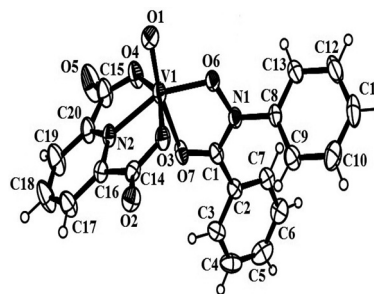


Fig. 2 Ortep view of complex **1**, [VO(PyDC)(BHA)], with the 25% ellipsoid probability.

Table 1 Selected bond lengths (Å) and bond angles (°) for the complexes

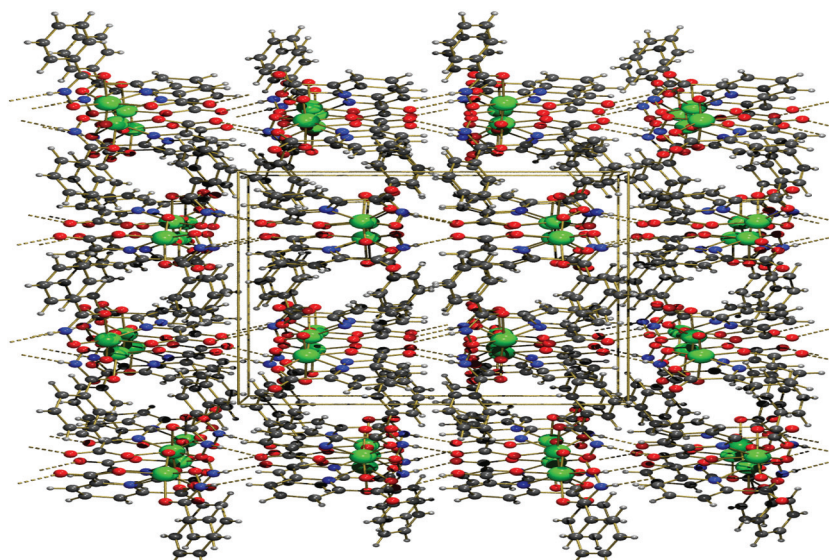
[VO(PyDC)(BHA)] (1)		[VO(PyDC)(BPHA)] (2)	
Bond distances:			
V(1)–O(1)	1.5804(16)	V(1)–O(1)	1.5770(17)
V(1)–N(2)	2.0422(14)	V(1)–N(2)	2.0548(17)
V(1)–O(7)	2.1594(13)	V(1)–O(7)	2.1471(15)
Bond angles:			
O(1)–V(1)–O(6)	94.31(7)	O(1)–V(1)–O(6)	93.52(7)
O(1)–V(1)–O(4)	96.60(7)	O(1)–V(1)–O(4)	94.31(8)
O(1)–V(1)–O(7)	169.92(7)	O(1)–V(1)–O(7)	165.50(8)
O(1)–V(1)–N(2)	102.84(7)	O(1)–V(1)–N(2)	108.03(8)

**Fig. 4** Ortep view of complex 2, [VO(PyDC)(BPHA)], with the 25% ellipsoid probability.

chain is formed due to strong hydrogen bonding (N1–H1...O2, 2.840 Å) between the hydrogen atom (H1) attached with the N atom of the coordinated BHA ligand with the carboxylate oxygen (O2) of the coordinated PyDC²⁻ ligand of another unit. Two anti-parallel zigzag chains are closely spaced through the cross-linked hydrogen bonding (C3–H3...O7, 2.830 Å) between aromatic hydrogen (H3) and carbonyl oxygen (O7) of hydroxamate ligands (BHA) of two different chains. Similarly, in complex 2 the packing structure (Fig. 5) shows that the two dimensional molecular layer is formed due to weak hydrogen bonding [(C18–H18...O5, 3.316(3) Å and (C11–H11...O2, 3.329(3) Å)] between aromatic hydrogen atoms (H18) and (H11) and carboxylate oxygen (O5) and carbonyl oxygen (O2) atoms of PyDC²⁻ and BPHA ligands respectively. In complex 2, the two essentially planar 2,6-pyridine dicarboxylate and benzophenylhydroxamate ligands are nearly orthogonal to each other, the dihedral angle between the least-square planes through the ligand atoms is 84.96° (1). In complex 1 the infinite 1D H-bonding is formed due to the presence of a N–H hydrogen of the primary hydroxamic acid ligand, which forms the supramolecular crystal packing network, whereas in complex 2, the N–H hydrogen of the BHA ligand is replaced by a phenyl group in the BPHA ligand and because of the presence of this phenyl

group, the formation of the extended H-bonding is hindered. The co-ligand PyDC²⁻ plays an important role in stabilizing the supramolecular packing in complex 2. Precisely, the carboxylate oxygen of the PyDC²⁻ ligand (O5 and H18–C18) formed an intermolecular H-bonding enclosing a ten-membered ring motif which can be designated through Etter's graph set notation as R²₂(10) (Fig. 5). All other important bond lengths and bond angles are given in Table 1 which are comparable to the corresponding values reported earlier for monomeric oxovanadium(v) complexes.⁵⁷ The tables of hydrogen bonding of both the complexes are provided as ESI.†

Peroxidative bromination of functionalized organic compounds. As the vanadium based active site structure of VHPO enzyme plays a key role in the biosynthesis of halogenated organic compounds *via* the oxidation of halides, the ability to mimic such a type of reaction by the newly synthesized oxovanadium(v) complexes has been examined for the bromination of phenol, *o*-cresol and *p*-cresol in the presence of H₂O₂ and KBr. Both complexes 1 and 2 have been found to catalyse the bromination reaction effectively in the presence of H₂O₂ though their efficiencies are different (Table 2). The mechanism of bromide oxidation may take place in a similar fashion

**Fig. 3** Extended H-bonding and packing arrangement of the complex [VO(PyDC)(BHA)] (1).

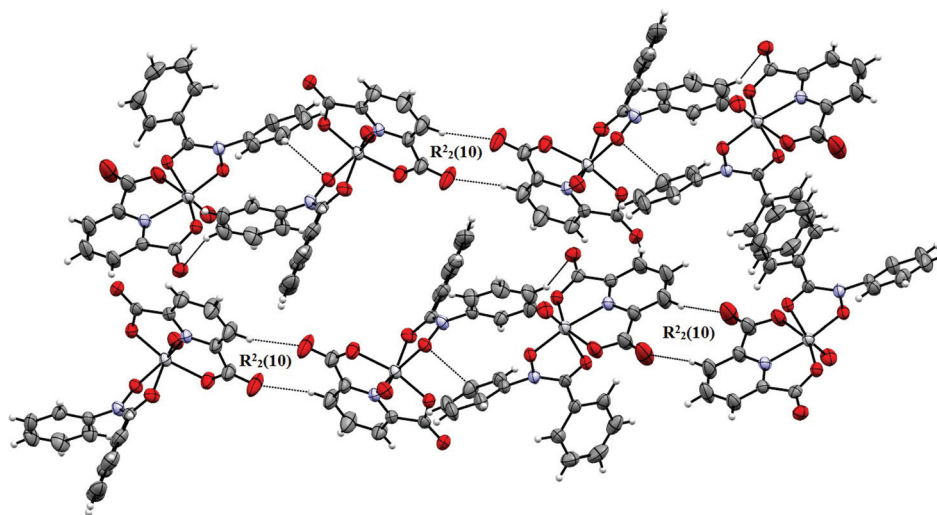


Fig. 5 H-bonding enclosing a ten-membered ring motif present in the unit cell of the crystal lattice of the complex [VO(PyDC)(BPHA)] (2).

Table 2 Details of the catalytic bromination of functionalized organic compounds in stirring^a acetonitrile using **1** and **2** as a catalyst^{b,c} in the presence of H₂O₂ as a terminal oxidant and KBr in acidic medium at room temperature

Entry	Substrate	Brominated products	% Yields of brominated products	
			Catalyst 1	Catalyst 2
1		 	69 A(1) B(17) C(51)	72 A(11) B(12) C(41)
2		 	50 D(4) E(14) F(32)	61 D(4) E(22) F(35)
3		 	45 G(20) H(25)	69 G(30) H(39)

^a24 h (entry 1), 20 h (entries 2 and 3). ^bBlank experiments were performed, *i.e.* dropping the catalyst alone while other additives and parameters remain the same. For entries 2 and 3 substrate bromination was found to be negligible. For entry 1 *ca.* 7% and 5% conversion took place for catalysts **1** and **2** respectively. ^cThe mole ratio of catalyst/substrate = 1 : 200 (entry 1 using catalyst **2**), 1 : 100 (entry 1 using catalyst **1** and entries 2 and 3).

as has been reported earlier,⁴³ and hence, in the present case, the oxovanadium(v) moiety of the complex is proposed to be converted to the hydroperoxovanadium(v) intermediate by reacting with H₂O₂ and subsequently this peroxide coordinated vanadium(v) intermediate oxidized the bromide (Br⁻) under mild acidic condition to a bromonium ion (Br⁺);⁴³

thereafter this *in situ* generated bromonium ion was trapped by suitable organic substrates as per the earlier proposition.⁴³ To get the optimum result, the pH of the reaction medium was adjusted⁵³ to ~3.0. Control experiments of the bromination reactions performed by maintaining all other additives and parameters fixed without the catalyst show that the yield of the brominated products is negligibly small after a long period of reaction, while in the presence of the catalysts, the percentage yield of the brominated products is appreciably high (Table 2). The results of the catalytic bromination reaction show that the efficiency of the bromination reaction is dependent on the nature of the catalyst which is governed by the ligand environment of the vanadium centre. The yield percentage of the brominated product in the case of the phenol substrate is maximum (69% for catalyst **1** and 72% for catalyst **2**) compared to *o*-cresol (50% for catalyst **1** and 61% for catalyst **2**) and *p*-cresol (45% for catalyst **1** and 69% for catalyst **2**). During the course of the catalytic bromination reaction, although other possible brominated products are obtained depending on the substrates, the mono brominated products are the major ones in the case of *ortho*-cresol and *para*-cresol, while in the case of phenol, the dibrominated one is the major product. So, it is observed that catalyst **1** is relatively less potent than catalyst **2**. It can be realised that the metal centre of catalyst **1** is coordinated with the hydroxamate moiety whereas catalyst **2** is coordinated with a secondary hydroxamate in which the hydrogen of the hydroxamate nitrogen is replaced by the phenyl group. Hence, the presence of the phenyl group in catalyst **2** might have induced higher reactivity of the hydroperoxovanadium(v) intermediate coordinated with the secondary hydroxamate ligand. The results of the GC-Mass analysis are included in the ESI.†

DNA binding study by absorption spectrophotometry. Electronic absorption spectroscopy is one of the useful techniques for monitoring the binding^{58,59} of metal complexes with DNA. The significant modification of the UV absorption band of both complexes **1** and **2** on the addition of increasing amounts

of DNA indicates the binding of both complexes **1** and **2** with DNA. Upon the addition of increasing amounts of CT DNA ($0\text{--}10^{-4}$ M) to complex **1** (10^{-4} M), the ligand based charge transfer band at 268 nm exhibited hyperchromism with a significant blue shift (5 nm). Such hyperchromism along with the concomitant blue shift in the spectra rules out groove binding and suggests an intimate association of complex **1** with CT DNA and it is likely that this complex **1** binds to CT DNA electrostatically *via* external contact (surface binding) with the DNA duplex.^{60,61} On the other hand, upon the addition of increasing amounts of CT DNA ($0\text{--}10^{-4}$ M) to complex **2** (10^{-4} M), the ligand based charge transfer band at 269 nm exhibited hypochromism with a significant red shift (5 nm). This indicates that there is an involvement of a strong stacking interaction between the aromatic chromophore of complex **2** and the DNA base pairs.^{59,62} This observation has further been supported by quantitative studies. Hypochromism results from the contraction of DNA helix as well as the conformational changes to DNA,^{16,63} while hyperchromism results from a change in the secondary structure of the DNA double helix.⁶⁴ The substantial difference in binding nature of the complexes could arise due to the presence of more planar rings in complex **2** in comparison to complex **1**. In order to quantitatively compare the binding strength of complexes **1** and **2** with CT DNA, the intrinsic binding constant (K_b) values were calculated following eqn (2) and were found to be $(1.34 \pm 0.2) \times 10^4$ and $(1.37 \pm 0.3) \times 10^5$ M⁻¹, for complexes **1** and **2** respectively. The higher K_b value of complex **2** is due to the benzophenyl-hydroxamic acid ligand which possesses a greater planar area, thereby leading to stronger binding within the DNA base pairs by the intercalative mode.⁶⁵ The K_b values of complexes **1** and **2** support the binding nature as suggested qualitatively from the change in intensity and position of UV bands. The K_b values revealed that complex **2** possesses a higher affinity for DNA binding in comparison to complex **1**. The corresponding results of absorbance spectral studies are provided as ESI.†

Fluorescence emission study for DNA interaction. The results obtained from spectrofluorometric titrations indicated that both complexes **1** and **2** could effectively bind to DNA. In order to confirm the binding mode and compare the binding affinities of the metal complexes to DNA, an ethidium bromide (EB) displacement experiment was carried out. Ethidium bromide is a weakly fluorescent compound, but its fluorescence is greatly increased when EB is specifically intercalated into the base pairs of double stranded DNA.⁶⁶ Further enhancement of the emission intensity of the CT-DNA-EB system with increasing concentrations ($0\text{--}10^{-4}$ M) of complex **1** is observed (Fig. 6). It is to be noted that complex **1** alone does not show any fluorescence in PBS buffer, but it induces an increase in the fluorescence of the DNA-EB complex. This effect could not be explained at this point. On the other hand, under the same experimental conditions, it is observed that there is a decrease in emission intensity of the CT-DNA-EB system with increasing concentration of complex **2** ($0\text{--}10^{-4}$ M) (Fig. 7). This may happen because either EB binds the metal complex strongly, resulting in a decrease in

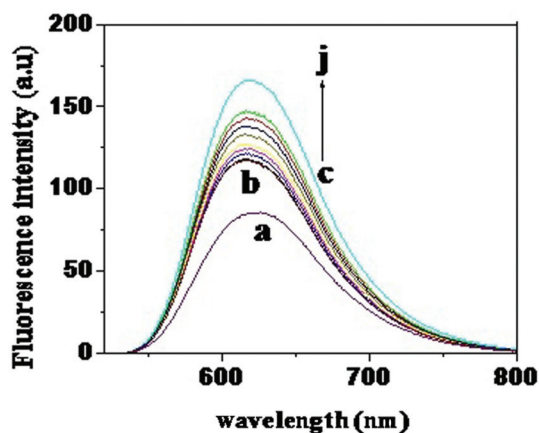


Fig. 6 Fluorescence spectra of (a) 1.25×10^{-4} M EB only, (b) EB + 10^{-4} M DNA control, and (c)–(j) EB + DNA + $(0.1\text{--}1.0) \times 10^{-4}$ M complex **1**. The arrow shows that the intensity increased with the concentration of complex **1**.

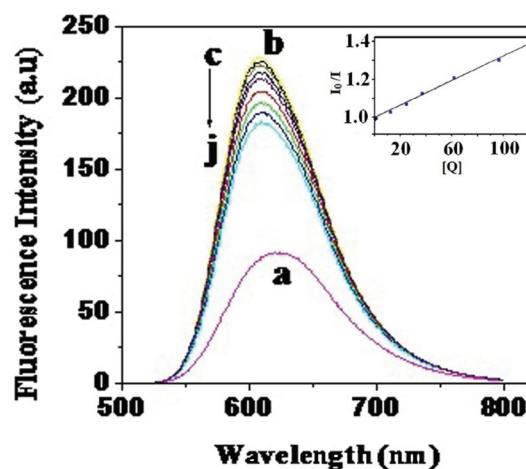


Fig. 7 Fluorescence spectra of (a) 1.25×10^{-4} M EB only, (b) EB + 10^{-4} M DNA control, and (c)–(j) EB + DNA + $(0.1\text{--}1.0) \times 10^{-4}$ M complex **2**. The arrow shows that the intensity decreased with the concentration of complex **2**. Inset: Stern-Volmer plot for the quenching of fluorescence of the ethidium bromide (EB) DNA complex caused by complex **2**.

the amount of EB intercalated into DNA, or there exists competitive intercalation between the metal complex and EB with DNA, thereby releasing some EB from the DNA-EB system.^{67,68} To get more straightforward information on the quenching of fluorescence intensity, the Stern-Volmer quenching constant K_{SV} was determined. The K_{SV} value was calculated from the plot of I_0/I versus $[Q]$. According to the linear Stern-Volmer equation,⁶⁹

$$I_0/I = 1 + K_{SV} [Q] \quad (1)$$

where I_0 and I are the fluorescence intensities in the absence and presence of a quencher $[Q]$ (Complex) respectively. K_{SV} is the Stern-Volmer quenching constant, which is obtained from the slope of the plot of I_0/I vs. $[Q]$. K_{SV} was given by the ratio of the slope to the intercept. The K_{SV} value for complex **2** is found to be $(1.72 \pm 0.3) \times 10^5$ M⁻¹ at 37 °C. These data suggest that

complex 2 binds strongly with CT-DNA. The high K_{sv} value indicates a strong binding of complex 2 with DNA by displacing the EB from DNA base pairs. This observation also supports the proposition from spectrophotometric studies [*vide* the K_b value of DNA-complex 2 which is $(1.37 \pm 0.3) \times 10^5 \text{ M}^{-1}$] that complex 2 binds the double stranded DNA by intercalation.

Gel electrophoresis study for nuclease activity. The efficiency of DNA cleavage activity of complexes 1 and 2 has been assessed by gel electrophoresis using super coil (SC) pUC 19 DNA in Tris-HCl-NaCl buffer ($5 \times 10^{-2} \text{ mL}^{-1}$, pH 7.2). The double-stranded plasmid pUC19 DNA exists in a compact super coil form. Upon induction of strand breaks, the super coil form of DNA is disrupted into the nicked coil (NC) form and the linear coil (LC) form. If one strand is cleaved, the super coil form will relax to produce a nicked coil form. If both the strands are cleaved, a linear coil form will be produced. A relatively fast migration is observed for the super coil form when the plasmid DNA is subjected to electrophoresis. The nicked coil form migrates slowly and the linear coil form migrates between SC and NC.⁷⁰ Hence, DNA strand breaks induced by complexes 1 and 2 were quantified by gel electrophoresis experiment by measuring the transformation of the super coil form into nicked coil and linear coil forms and the results are presented in Fig. 8 and 9 respectively. The control experiment suggests that untreated DNA (lane 1) has 86% form I (SC) and 14% form II (NC). The treatment of DNA with $(1-5) \times 10^{-6}$ mol of complex 1 produces 17–36% of form II (NC) and 17–24% of form III (LC), *i.e.* complex 1 induces up to

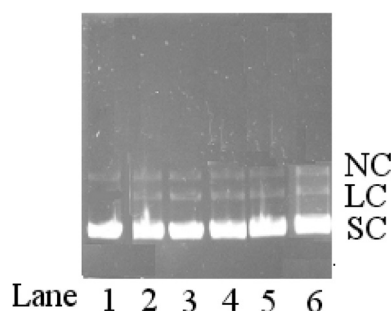


Fig. 8 Cleavage of super coil pUC19 DNA (150 ng) by complex 1 in Tris-HCl buffer ($5 \times 10^{-2} \text{ mL}^{-1}$, pH 7.2) containing $5 \times 10^{-2} \text{ mL}^{-1}$ NaCl at 37 °C for an hour. Lane 1: DNA control, lanes 2–6: DNA + $(1-5) \times 10^{-6}$ M of complex 1. SC: super coil, NC: nicked coil and LC: linear coil.

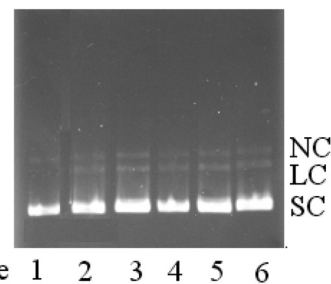


Fig. 9 Cleavage of super coil pUC19 DNA (150 ng) by complex 2 in Tris-HCl buffer ($5 \times 10^{-2} \text{ mL}^{-1}$, pH 7.2) containing $5 \times 10^{-2} \text{ mL}^{-1}$ NaCl at 37 °C for an hour. Lane 1: DNA control, lane 2–6: DNA + $(1-5) \times 10^{-6}$ M of complex 2. SC: super coil, NC: nicked coil and LC: linear coil.

60% nicking in plasmid DNA, whereas under the same experimental conditions, complex 2 produces 20–41% of form II (NC) and 18–30% of form III (LC), *i.e.* thereby induces up to 71% nicking (Table 3). It may be noted that the metal ion or the ligand alone are not capable of inducing any cleavage in the plasmid DNA. It is evident from the above experiments that complex 2 has greater efficiency of cleaving SC DNA (form I) into NC (form II) and LC (form III) than complex 1. This may be a result of the involvement of the extended aromatic ring of the BPHA ligand^{71,72} in partial intercalation with DNA, which in turn facilitates nicking.

Conclusions

In the present communication, the design, synthesis and biomimicking activity of two oxovanadium complexes have been presented, where complex 1 has the hydroxamate group and complex 2 is having a secondary hydroxamate group. The complexes were tested for bromoperoxidation activity. It is found that both the complexes are capable to oxidatively brominate the phenol, *o*-cresol and *p*-cresol, thereby mimicking the role of the vanadium based bromoperoxidase enzyme. The nuclease activity of both the complexes has been demonstrated with pUC19 DNA. The gel electrophoregram and subsequent analysis show that the complexes induce substantial nicking in the DNA strand, thereby producing both nicked coil (NC II) and linear coil (LC III) forms of DNA. So, the two structurally characterized oxovanadium(v) complexes can catalyse the peroxidative bromination of organic substrates in general, and

Table 3 Extent of DNA SC pUC19 (150 ng) cleavage by complexes 1 and 2

Lane no.	Reaction conditions	Complex 1			Complex 2		
		Form I (% SC)	Form II (% NC)	Form III (% LC)	Form I (% SC)	Form II (% NC)	Form III (% LC)
1	DNA control	86	14	0	86	14	0
2	DNA + 1 μM complex	66	17	17	62	20	18
3	DNA + 2 μM complex	56	21	23	55	23	22
4	DNA + 3 μM complex	54	23	23	45	31	24
5	DNA + 4 μM complex	52	24	24	35	36	29
6	DNA + 5 μM complex	40	36	24	29	41	30

phenol and phenol derivatives in particular, and also exhibit nuclease activity by inducing nicking in the super coil (SC) DNA.

Experimental

Materials

Ammonium metavanadate and sodium bicarbonate were of extrapure variety and purchased from SRL, India and were used directly. Pyridine-2,6-dicarboxylic acid was obtained from Avra, India. Extrapure zinc dust, *o*-cresol and *p*-cresol were obtained from Loba Chemie (India). Nitrobenzene and benzoyl chloride were obtained from B.D.H. (India). Liquid ammonia was obtained from Ranbaxy (India). All the other chemicals needed were obtained from Merck (India). Acetonitrile, dichloromethane and acetone were further purified by a literature method⁷³ for physicochemical studies. Ultra high pure grade dioxygen, dihydrogen, zero air and dinitrogen gas used for chromatographic analysis were obtained from Indian Refrigeration Stores, Calcutta. The ligands benzohydroxamic acid and *N*-benzophenylhydroxamic acid were prepared as described previously^{74,75} and characterized by elemental analysis, UV-vis spectroscopy, IR, mass and ¹H NMR spectral studies. All the solvents used for chromatographic analysis were either of HPLC, spectroscopic or GR grade and in all cases their purity was confirmed by GC analysis before use. CT DNA was obtained from the Sigma Chemical Company, USA and super coil plasmid pUC19 DNA was procured from Genei (Bangalore, India).

Physical measurements

Infrared spectra were recorded as KBr pellets using a Perkin-Elmer RFX-I spectrophotometer and electronic spectra were taken using an Agilent 8453E UV-vis spectrophotometer using a 1 cm quartz cell against an appropriate reagent blank. Elemental analyses were performed using a Perkin Elmer 2400 series II CHNS analyzer. The conductances of 10⁻³ (M) solutions were measured using a Systronics 304 Conductivity Meter. Magnetic susceptibility measurements were made using a Magway MSB MKI Magnetic Susceptibility Balance (Sherwood Scientific Ltd, Cambridge, England) at 298 K. NMR spectra were recorded at room temperature using a Bruker 300 MHz NMR spectrometer. Mass spectra were obtained using a Qtof Micro YA263 mass spectrometer. GC measurements were made either on an Agilent 6890N gas chromatograph using HP-1 and INNOWAX capillary column in the FID mode with dinitrogen as the carrier gas or a SHIMADZU-QP-5050A spectrometer whereas GC-MS measurements were made using a SHIMADZU-QP-5050A spectrometer.

Synthesis of the ligand, benzohydroxamic acid (BHAH)

The ligand was prepared as described previously.⁷⁴ Yield: 1.1 g (80%). Anal. Calc. for C₇H₇O₂N: C - 61.3, H - 5.1, N - 10.2. Found: C - 61.4, H - 5.1, N - 10.2%. IR (KBr, cm⁻¹): 3254(m): ν_(N-H), 1608(s): ν_(C=O), 1487(w): ν_(C-N), 920(w): ν_(N-O). ¹H NMR

(300 MHz, CD₃OD, δ ppm): 7.7–7.4 (5H, m, aromatic protons). UV-vis: λ_{max}, nm (ε, M⁻¹ cm⁻¹): 223 (7790). The structural representation of the ligand benzohydroxamic acid (BHAH) is shown in Fig. 1.

Synthesis of the ligand, *N*-benzophenylhydroxamic acid (BPHAH)

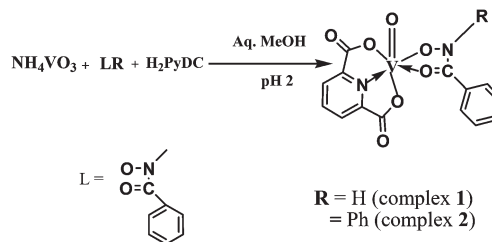
The ligand was prepared as described previously.⁷⁵ Yield: 1.5 g (70%). Anal. Calc. for C₁₃H₁₁O₂N: C - 73.2, H - 5.2, N - 6.6. Found: C - 73.2, H - 5.1, N - 6.6%. IR (KBr, cm⁻¹): 1623(s): ν_(C=O), 1491(w): ν_(C-N), 925(w): ν_(N-O). ¹H NMR (300 MHz, CD₃OD, δ ppm): 7.4–7.2 (10H, m, aromatic protons): 9.1(1H, s, from N(ph)-OH). UV-vis: λ_{max}, nm (ε, M⁻¹ cm⁻¹): 267 (15 128). The structural representation of the ligand benzophenyl hydroxamic acid (BPHAH) is shown in Fig. 1.

Synthesis of the complex [VO(PyDC)(BHA)] (1)

NH₄VO₃ (58 mg *i.e.* 5 × 10⁻⁴ mol) was dissolved in warm water with constant stirring and acidified with dilute HCl, then 84 mg, *i.e.* 5 × 10⁻⁴ mol aqueous solution of H₂PyDC was added followed by the addition of a 15 mL methanolic solution of BHAH (69 mg *i.e.* 5 × 10⁻⁴ mol). Immediately, a deep purple precipitate of complex 1 was obtained (Scheme 1). The precipitate was filtered off and washed with water. The compound is soluble in dichloromethane, chloroform, acetone, acetonitrile and methanol and is a nonelectrolyte. Single crystals suitable for X-ray diffraction were obtained by the slow diffusion of complex 1 in an acetone–petroleum ether mixture. It is air stable and diamagnetic at 298 K. Yield: 135 mg (64%). Anal. Calc. for C₁₄H₉N₂O₇V: C - 45.7, H - 2.5, N - 7.6. Found: C - 45.6, H - 2.4, N - 7.6%. IR (KBr disc, cm⁻¹): 1674(s): ν_{asym}(COO⁻), 1603(m): ν_(C-O), 1557(m): ν_{sym}(COO⁻), 1485(m): ν_(C-N), 989(s): ν_(V=O), 914(m): ν_(N-O). UV-vis: λ_{max}, nm (ε, M⁻¹ cm⁻¹): 268 (6428), 222 (11 930). MS: *m/z* 368. ¹H NMR (300 MHz, CDCl₃, δ ppm): 8.7–8.3 (3H, m, H₂PyDC), 7.8–7.5 (5H, m, aromatic protons of BHAH).

Synthesis of the complex [VO(PyDC)(BPHA)] (2)

NH₄VO₃ (58 mg *i.e.* 5 × 10⁻⁴ mol) was dissolved in warm distilled water with constant stirring and acidified with dilute HCl, then 84 mg, *i.e.* 5 × 10⁻⁴ mol aqueous solution of H₂PyDC was added followed by the addition of a 15 mL methanolic solution of BPHAH (106 mg *i.e.* 5 × 10⁻⁴ mol), while a reddish brown precipitate of complex 2 was obtained (Scheme 1). The



Scheme 1 The synthetic pathway of the oxovanadium(v) complexes [VO(PyDC)(BHA)] (1) and [VO(PyDC)(BPHA)] (2).

product was filtered off, washed several times with water and finally dried in vacuum. The compound is soluble in dichloromethane, chloroform, acetone, acetonitrile and methanol and behaves as a nonelectrolyte. Single crystals suitable for X-ray diffraction studies were obtained by the slow diffusion of a dichloromethane solution of complex 2 in hexane. Complex 2 is air stable and diamagnetic at 298 K. Yield: 150 mg (60%). Anal. Calc. for $C_{20}H_{13}N_2O_7V$: C – 54.1, H – 3.0, N – 6.3. Found: C – 54.0, H – 2.9, and N – 6.3%. IR (KBr disc, cm^{-1}): 1700(s); $\nu_{asym}(COO^-)$, 1598(m); $\nu_{(C-O)}$, 1537(w); $\nu_{asym}(COO^-)$, 1488(w); $\nu_{(C-N)}$, 987(s); $\nu_{(v=O)}$, 918(m); $\nu_{(N-O)}$. UV-vis: λ_{max} , nm (ϵ , $M^{-1} cm^{-1}$): 269 (10 754), 225 (20 700). MS: m/z 444. 1H NMR (300 MHz, $CDCl_3$, δ ppm): 8.5 (1H, t, $J = 7.7$ Hz), 8.3 (2H, d, $J = 7.5$ Hz), 7.6–7.2 (10H, m, aromatic protons). ^{13}C NMR (75 MHz, $CDCl_3$, δ ppm): 166.7, 150.9, 146.3, 139.8, 133.0, 130.6, 129.7, 129.5, 128.7, 128.5, 127.5, 127.4, 126.1. The synthetic pathway of complex 2 is shown in Scheme 1.

X-ray structure analysis for complexes 1 and 2

Single crystals of $[VO(PyDC)(BHA)]$ (1) and $[VO(PyDC)(BPHA)]$ (2) were obtained by slow diffusion of an acetone solution of complex 1 in petroleum ether and a dichloromethane solution of complex 2 in hexane respectively. Selected crystal data and data collection parameters are given in Table 4. Data were collected on a Bruker SMART Apex CCD area detector using graphite monochromated Mo $K\alpha$ radiation ($\lambda = 0.71073 \text{ \AA}$). X-ray data reduction, structure solution and refinement were

done using SHELXS-97 and SHELXL-97 programs.⁷⁶ The structures were solved by a direct method.

Experimental set-up for catalytic bromination

A mixture of complex 1 (the catalyst) (8.8 mg, *i.e.* 2.4×10^{-5} mol), and a representative substrate, namely phenol (226.2 mg, *i.e.* 2.4×10^{-3} mol; for the other cases see Table 2), was dissolved in a 5.0 mL CH_3CN solvent and the solution was taken in a 100 mL stoppered conical flask. To the above solution, 1.0 mL aqueous solution of KBr (589.2 mg, *i.e.* 4.8×10^{-3} mol) and 1.0 mL (9.8×10^{-3} mol) of 30% H_2O_2 were added under stirring conditions. The pH of the resulting solution was adjusted to 3 by adding 2 M nitric acid. The resulting yellow solution was stirred continuously at room temperature for 24 h followed by quantitative extraction of the organic part with 2.0 mL of diethyl ether so that practically the entire reaction product was transferred to the ether layer. Thereafter, the ether extract was concentrated to ~ 1.0 mL by slow evaporation. From the extract, 1.0 μ L of the solution was taken in a gas syringe and injected through a GC port. The same method was adopted in the case of the reaction with catalyst 2 except that complex 2 was added in place of complex 1. The products were characterized by GC-MS spectrometry.

DNA binding measurements

UV-vis spectral study. Absorption spectral titration experiments were performed by monitoring a 268 nm band for complex 1 and 269 nm for complex 2 in the respective cases. In each case the concentration of the complex was maintained at 10^{-4} M, while the concentration of the CT DNA was varied between the range of $(0.2\text{--}1.0) \times 10^{-4}$ M. An appropriate quantity of CT DNA was added to both the complex solution and the reference solution to eliminate the absorbance of DNA itself. From the absorption data, the intrinsic binding constant K_b was determined from a plot of $[DNA]/(\epsilon_a - \epsilon_f)$ vs. $[DNA]$ using the equation:

$$[DNA]/(\epsilon_a - \epsilon_f) = [DNA]/(\epsilon_b - \epsilon_f) + 1/K_b (\epsilon_b - \epsilon_f) \quad (2)$$

where $[DNA]$ is the concentration of DNA in base pairs. The apparent absorption coefficients ϵ_a , ϵ_f and ϵ_b correspond to $A_{obsd}/[complex]$, the extinction coefficient for the free V-complex and the extinction coefficient for the V-complex in the fully bound form, respectively. Plots of $[DNA]/(\epsilon_a - \epsilon_f)$ versus $[DNA]$ gave a slope $1/(\epsilon_b - \epsilon_f)$ with intercept $1/K_b (\epsilon_b - \epsilon_f)$, where K_b is obtained from the slope to the intercept ratio.

Fluorescence emission study. Emission intensity measurements were carried out using an RF-5301PC Shimadzu spectrofluorimeter. In this binding experiment, 50 μ L of a CT DNA (10^{-4} M) solution in Tris-HCl-NaCl buffer (5×10^{-2} mol Tris-HCl and 5×10^{-2} mol NaCl, pH 7.2) was added to 2.0 mL of ethidium bromide (1.25×10^{-4} M) in the same buffer medium to get the maximum fluorescence intensity. Aliquots of 10^{-3} M stock solution of the complex in DMF were added to the ethidium bromide bound CT DNA solution and the fluorescence was measured for each test solution after 2 hours of incubation

Table 4 Crystal data and structure refinement parameters for the complexes $[VO(PyDC)(BHA)]$ (1) and $[VO(PyDC)(BPHA)]$ (2)

Parameters	$[VO(PyDC)(BHA)]$	$[VO(PyDC)(BPHA)]$
Molecular formula	$C_{14}H_9N_2O_7V$	$C_{20}H_{13}N_2O_7V$
Formula weight	368.17	444.26
Crystal system	Orthorhombic	Monoclinic
Space group	<i>Pbcn</i> (no. 60)	<i>P21/n</i>
a, b, c [\AA] α, β, γ [$^\circ$]	16.9290(13), 11.0728(9), 15.1442(12), 90, 90, 90	12.3056(3), 6.0449(2), 26.4794(6), 90, 102.664(2), 90
V [\AA^3], Z	2838.8(4), 8	1921.78(9), 4
D_{calc} . [$g\text{ cm}^{-3}$]	1.723	1.535
μ [mm^{-1}]	0.742	0.563
$F(000)$	1488	904
Crystal size [mm]	$0.05 \times 0.05 \times 0.30$	$0.20 \times 0.05 \times 0.04$
Data collection		
Temperature (K)	273	293
Radiation [\AA] MoK α	0.71073	0.71073
Φ Range [$^\circ$]	2.41, 27.45	1.58, 27.55
Dataset	–21: 21, –13: 14, –19: 19	–16: 15, –7: 7, –34: 34
Tot., uniq. data, $R(int)$	21460, 3236, 0.0949	16721, 4414, 0.039
Observed data [$I > 2.0\sigma(I)$]	2679	3193
Refinement		
N_{ref}, N_{par}	3236, 217	4414, 271
R, wR_2, S	0.0359, 0.1180, 0.818	0.039, 0.1019, 1.034
$w = 1/[s^2(F_o^2) + (0.0710P)^2]$ where $P = (F_o^2 + 2F_c^2)/3$		
Max. and av. shift/error	0.001, 0.000	0.00, 0.00

at 37 °C. The solutions were excited at 515 nm (with excitation and emission slit 3 nm) and emission spectra were recorded from 520 to 800 nm. The solutions containing an equivalent amount of a CT DNA solution and either complex 1 or complex 2 and buffer when excited at 515 nm did not exhibit any fluorescence emission.

Gel electrophoresis study. The stock solution of supercoiled pUC19 DNA (5 µL, 150 ng) in Tris-HCl buffer ($5 \times 10^{-2} \text{ mL}^{-1}$, pH 7.2) containing $5 \times 10^{-2} \text{ mL}^{-1}$ NaCl (20 µL) was prepared. From the stock solution, a 2 µL aliquot was treated with the appropriate metal complex (stock solution 2 mL, $4 \times 10^{-2} \text{ mL}^{-1}$) followed by dilution with Tris-HCl buffer to a total volume of 20 µL. The samples were then incubated for an hour at 37 °C, loading buffer containing 25% bromophenol blue and 30% glycerol (3 µL) was added and loaded on 0.9% agarose gel containing 10^{-3} mL^{-1} EB. Electrophoresis was carried out at 40 V for 2 h in TAE buffer ($4 \times 10^{-2} \text{ mL}^{-1}$ Tris, $2 \times 10^{-2} \text{ mL}^{-1}$ acetic acid, and 10^{-3} mL^{-1} EDTA, pH 7.2). The gel electrophoregrams were photographed using a UVP-Bio-Doc-It Gel documentation setup coupled with a CCD camera. The extent of super coil (SC) pUC19 DNA cleavage induced by either complex 1 or complex 2 was determined by analysing the intensities of the bands using UVP Doc It LS 2.0 Gel Documentation Software.

Acknowledgements

The authors wish to extend their thanks to UGC for funding in the form of a Major Research Project to KKM [Sanction no. F.NO. 39-706/2010(SR)]. The authors are thankful to Jadavpur University for facilities. The NMR and X-ray diffractometer used in this work were funded by DST, India in the form of DST-FIST to the Department of Chemistry, Jadavpur University. T. K. S. is thankful to CSIR, India for a Research Associateship (Award No. 9/96(0624)2K10-EMRI). The authors are thankful to Md Selim and Shiv Shankar Paul for assistance.

References

- D. Rehder, *Future Med. Chem.*, 2012, **4**, 1823–1837.
- (a) J. Nilsson, E. Degerman, M. Haukka, G. C. Lisensky, E. Garribba, Y. Yoshikawa, H. Sakurai, E. A. Enydy, T. Kiss, H. Esbak, D. Rehder and E. Norlander, *Dalton Trans.*, 2009, 7902–7911; (b) I. Correia, T. Jakusch, E. Cobbinna, S. Mehtab, I. Tomaz, N. V. Nagy, A. Rockenbauer, J. C. Pessoa and T. Kiss, *Dalton Trans.*, 2012, **41**, 6477–6487.
- N. Muhammad, S. Ali, S. Shahzadi and A. N. Khan, *Russ. J. Coord. Chem.*, 2008, **34**, 448–453.
- P. Noblia, M. Vieites, B. S. Parajon-Costa, E. J. Baran, H. Cerecetto, P. Draper, M. González, O. E. Piro, E. E. Castellano, A. Azqueta, A. L. deCeraín, A. Monge-Vega and D. Gambino, *J. Inorg. Biochem.*, 2005, **99**, 443–451.
- V. L. Pecoraro, C. Slebodnick and B. Hamstra, 1998 *Vanadium complexes: Chemistry, biochemistry and therapeutic applications* (ACS Symposium Series), ed. D. C. Crans and A. S. Tracy, Washington, DC, Am. Chem. Soc., ch. 12.
- D. Rehder, *Chem. Unserer Zeit*, 2010, **44**, 322–321.
- A. G. J. Ligtenbarg, R. Hage and B. L. Feringa, *Coord. Chem. Rev.*, 2003, **237**, 89–101.
- V. Conte, F. D. Furia and G. Licini, *Appl. Catal., A*, 1997, **157**, 335–361.
- (a) P. Adao, J. C. Pessoa, R. T. Henriques, M. L. Kuznetsov, F. Avecilla, M. R. Maurya, U. Kumar and I. Correia, *Inorg. Chem.*, 2009, **48**, 3542–3561; (b) H. H. Monfared, S. Alavi, A. Farrokhi, M. Vahedpour and P. Mayer, *Polyhedron*, 2011, **30**, 1842–1848; (c) M. R. Maurya, A. Kumar, P. Manikandan and S. Chand, *Appl. Catal., A*, 2004, **277**, 45–53; (d) K. C. Gupta and A. K. Sutar, *Coord. Chem. Rev.*, 2008, **252**, 1420–1450.
- A. Butler, M. J. Clague and G. E. Meister, *Chem. Rev.*, 1994, **94**, 625–638.
- A. Butler, *Bioinorganic catalysis*, ed. J. Reedijk and E. Bouwman, Marcel Dekker, New York, 2nd edn, 1999, ch. 5.
- D. C. Crans, J. J. Smee, E. Gaidamauskas and L. Yang, *Chem. Rev.*, 2004, **104**, 849–902.
- M. Mad'arová, M. Sivák, L. Kuchta, J. Marek and J. Benko, *Dalton Trans.*, 2004, 3313–3320.
- M. I. Isupov, A. R. Dalby, A. A. Brindley, Y. Izumi, T. Tanabe, G. N. Murshudov and J. A. Littlechild, *J. Mol. Biol.*, 2000, **299**, 1035–1049.
- A. Messerschmidt and R. Wever, *Proc. Natl. Acad. Sci. U. S. A.*, 1996, **93**, 392.
- T. K. Si, S. S. Paul, M. G. B. Drew and K. K. Mukherjea, *Dalton Trans.*, 2012, **41**, 5805–5815.
- J. Hartung, Y. Dumont, M. Greb, D. Hach, F. Kohler, H. Schulz, M. Časny, D. Rehder and H. Vilter, *Pure Appl. Chem.*, 2009, **81**, 1251–1264.
- G. J. Colpas, B. J. Hamstra, J. W. Kampf and V. L. Pecoraro, *J. Am. Chem. Soc.*, 1996, **118**, 3469–3478.
- M. R. Maurya, S. Sikarwar, T. Joseph, P. Manikandan and S. B. Halligudi, *React. Funct. Polym.*, 2005, **63**, 71–83.
- J. Kaizer, E. J. Klinker, N. Y. Oh, J. U. Rohde, W. J. Song, A. Stubna, J. Kim, E. Munck, W. Nam and L. Que Jr., *J. Am. Chem. Soc. (Commun.)*, 2004, **126**, 472–473.
- D. Kumar, H. Hirao, L. Que Jr. and S. Shaik, *J. Am. Chem. Soc. (Commun.)*, 2005, **127**, 8026–8027.
- A. Butler and J. N. Carter-Franklin, *Nat. Prod. Rep.*, 2004, **21**, 180–188.
- S. Tanaka, H. Yamamoto, H. Nozaki, K. B. Sharpless, R. C. Michaelson and J. D. Cutting, *J. Am. Chem. Soc.*, 1974, **96**, 5254–5255.
- H. Mimoun, L. Saussine, E. Daire, M. Postel, J. Fischer and R. Weiss, *J. Am. Chem. Soc.*, 1983, **105**, 3101–3110.
- D. A. Cogan, G. Liu, K. Kim, B. J. Backes and J. A. Ellman, *J. Am. Chem. Soc.*, 1998, **120**, 8011–8019.
- H. B. ten-Brink, A. Tuynman, H. L. Dekker, W. Hemrika, Y. Izumi, T. Oshiro, H. E. Schoemaker and R. Wever, *Inorg. Chem.*, 1998, **37**, 6780–6784.

- 27 Y. Hoshino and H. Yamamoto, *J. Am. Chem. Soc.*, 2000, **122**, 10452–10453.
- 28 G. V. Nizova, G. Süß-Fink, S. Stanislas and G. B. Shul'pin, *Chem. Commun.*, 1998, 1885–1886.
- 29 Y. Maeda, N. Kakiuchi, S. Matsumura, T. Nishimura and S. Uemura, *Tetrahedron Lett.*, 2001, **42**, 8877–8879.
- 30 T. S. Smith and V. L. Pecoraro, *Inorg. Chem.*, 2002, **41**, 6754–6760.
- 31 S.-H. Hsieh, Y.-P. Kuo and H.-M. Gau, *Dalton Trans.*, 2007, 97–106, DOI: 10.1039/b613212j.
- 32 A. D. N. Brenno and A. M. L. Alexandre, Recent Developments in the Chemistry of Deoxyribonucleic Acid (DNA) Intercalators: Principles, Design, Synthesis, Applications and Trends, *Molecules*, 2009, **14**, 1725–1746.
- 33 N. Margiotta, C. Marzano, V. Gandin, D. Osella, M. Ravera, E. Gabano, J. A. Platts, E. Petruzzella, J. D. Hoeschele and G. Natile, *J. Med. Chem.*, 2012, **55**, 7182–7192.
- 34 A. R. Banerjee, J. A. Jaeger and D. H. Turner, *Biochemistry*, 1993, **32**, 153–163.
- 35 N. Y. Sardesai, K. Zimmerman and J. K. Barton, *J. Am. Chem. Soc.*, 1994, **116**, 7502–7508.
- 36 J. Chen, J. Christiansen, R. C. Tittsworth, B. J. Hales, S. J. George, D. Coucouvanis and S. P. Cramer, *J. Am. Chem. Soc.*, 1993, **115**, 5509–5515.
- 37 K. H. Thompson and C. Orvig, *Coord. Chem. Rev.*, 2001, **219**, 1033–1053.
- 38 R. Olar, A. Dogaru, D. Marinescu and M. Badea, *J. Therm. Anal. Calorim.*, 2012, **110**, 257–262.
- 39 D. W. J. Kwong, O. Y. Chan, R. N. S. Wong, S. M. Musser, L. Vaca and S. I. Chan, *Inorg. Chem.*, 1997, **36**, 1276–1277.
- 40 M. Sam, J. H. Hwang, G. Chanfreau and M. M. Abu-Omar, *Inorg. Chem.*, 2004, **43**, 8447–8455.
- 41 R. K. Narla, Y. Dong, O. J. D'Cruz, C. Navara and F. M. Uckun, *Clin. Cancer Res.*, 2000, **6**, 1546–1556.
- 42 D. C. Crans, B. Zhang, E. Gaidamauskas, A. D. Keramidias, G. R. Willsky and C. R. Roberts, *Inorg. Chem.*, 2010, **49**, 4245–4256.
- 43 M. R. Maurya, S. Agarwal, C. Bader, M. Ebel and D. Rehder, *Dalton Trans.*, 2005, 537–544.
- 44 P. K. Sasmal, S. Saha, R. Majumdar, S. De, R. R. Dighe and A. R. Chakravarty, *Dalton Trans.*, 2010, **39**, 2147–2158.
- 45 (a) H. Sakurai, M. Nakai, T. Miki, K. Tsuchiya, J. Takada and R. Matsushita, *Biochem. Biophys. Res. Commun.*, 1992, **189**, 1090–1095; (b) D. W. J. Kwong, O. Y. Chan, R. N. S. Wong, S. M. Musser, L. Vaca and S. I. Chan, *Inorg. Chem.*, 1997, **36**, 1276–1277.
- 46 C. Hiort, J. Goodisman and J. C. Dabrowiak, *Biochemistry*, 1996, **35**, 12354–12362.
- 47 J. Benítez, L. Guggeri, I. Tomaz, J. C. Pessoa, V. Moreno, J. Lorenzo, F. X. Avilés, B. Garat and D. Gambino, *J. Inorg. Biochem.*, 2009, **103**, 1386–1394.
- 48 L. G. Naso, E. G. Ferrer, N. Butenko, I. Cavaco, L. Lezama, T. Rojo, S. B. Etcheverry and P. A. M. Williams, *J. Biol. Inorg. Chem.*, 2011, **16**, 653–668.
- 49 P. Carnoma, *Spectrochim. Acta*, 1980, **36A**, 705–712.
- 50 A. C. Gonzalez-Baro, E. E. Castellano, O. E. Piro and B. S. Parajón-Costa, *Polyhedron*, 2005, **24**, 49–55.
- 51 S. K. Dutta, E. R. T. Tiekink and M. Chaudhury, *Polyhedron*, 1997, **16**, 1863–1871.
- 52 C. N. R. Rao and R. Vekatraghavan, *Spectrochim. Acta*, 1962, **18**, 273–278.
- 53 T. K. Si, M. G. B. Drew and K. K. Mukherjea, *Polyhedron*, 2011, **30**, 2286–2293.
- 54 R. M. Silverstein, G. C. Bassler and T. C. Morrill, *Spectroscopic Identification of Organic Compounds*, John Wiley and Sons, New York, 1981.
- 55 H. H. Monfared, S. Kheirabadi, N. A. Lalami and P. Mayer, *Polyhedron*, 2011, **30**, 1375–1384.
- 56 D. Neculai, A. M. Neculai, H. W. Roesky, R. H. Irmer, B. Walfort and D. Stalke, *Dalton Trans.*, 2003, 2831–2834.
- 57 (a) Y. Jin, H.-I. Lee, M. Pyo and M. S. Lah, *Dalton Trans.*, 2005, 797–803, DOI: 10.1039/B500169M; (b) J. Gatjens, B. N. Meier, T. Kiss, E. M. Nagy, P. Buglyo, H. Sakurai, K. Kawabe and D. Rehder, *Chem.-Eur. J.*, 2003, **9**, 4924–4935.
- 58 S. R. Chowdhury, M. Selim, S. Chatterjee, S. Igarashi, Y. Yukawa and K. K. Mukherjea, *J. Coord. Chem.*, 2012, **65**, 3469–3480.
- 59 M. Selim and K. K. Mukherjea, *J. Biomol. Struct. Dyn.*, 2009, **26**, 561–566.
- 60 *Nucleic Acids in Chemistry and Biology*, ed. G. M. Blackburn and M. J. Gait, Oxford University Press, New York, 2nd edn, 1996, p. 329.
- 61 F. Arjmand, M. Muddassir and R. H. Khan, *Eur. J. Med. Chem.*, 2010, **45**, 3549–3557.
- 62 J. Lu, Y. Du, H. Guo, J. Jiang, X. Zeng and L. Zang, *J. Coord. Chem.*, 2011, **64**, 1229–1239.
- 63 P. K. Sasmal, R. Majumdar, R. R. Dighe and A. R. Chakravarty, *Dalton Trans.*, 2010, **39**, 7104–7113.
- 64 R. Eshkourfu, B. Čobeljić, M. Vujčić, I. Turel, A. Pevec, K. Sepčić, M. Zec, S. Radulović, T. Srdić-Radić, D. Mitić, K. Andjelković and D. Sladić, *J. Inorg. Biochem.*, 2011, **105**, 1196–1203.
- 65 R. Indumathy, M. Kanthimathi, T. Weyhermuller and B. U. Nair, *Polyhedron*, 2008, **27**, 3443–3450.
- 66 M. Selim, S. R. Chowdhury and K. K. Mukherjea, *Int. J. Biol. Macromol.*, 2007, **41**, 579–583.
- 67 F. Arjmand and S. Parveen, *RSC Adv.*, 2012, **2**, 6354–6362.
- 68 G. Zhang, J. Guo, J. Pan, X. Chen and J. Wang, *J. Mol. Struct.*, 2009, **923**, 114–119.
- 69 M. R. Efinck and C. A. Ghiron, *Anal. Biochem.*, 1981, **114**, 199–227.
- 70 C. Li, H. Tian, S. Duan, X. Liu, P. Xu, R. Qiao and Y. Zhao, *J. Phys. Chem. B*, 2011, **115**, 13350–13354.
- 71 J. Li, J. Dong, H. Cui, T. Xu and L. Li, *Transition Met. Chem.*, 2012, **37**, 175–182.
- 72 S. Ramakrishnan, D. Shakthipriya, E. Suresh, V. S. Periasamy, M. A. Akbarsha and M. Palaniandavar, *Inorg. Chem.*, 2011, **50**, 6458–6471.
- 73 G. H. Jeffery, J. Bassett, J. Mendham and R. C. Denny Addison, *Vogel's Text Book of Quantitative Chemical Analysis*, Wesley Longman Limited, UK, 5th edn, 1989.

- 74 C. R. Hauser and W. B. Renfrow, *Org. Synth.*, 1943, 2(67), 1939, 19, 15.
- 75 (a) A. K. Majumdar, in *N-benzophenyl Hydroxylamine and its Analogs*, ed. R. Belcher, A. Frieser, Pergamon Press, Braunschweig, 1971 and references cited therein;
(b) R. C. Mehrotra, in *Comprehensive Coordination Chemistry*, ed. G. Wilkinson, R. D. Gillard, J. A. McCleverty, Pergamon Press, New York, 1987, vol. 1 and references cited therein.
- 76 G. M. Sheldrick, *SHELXS-97 and SHELXL-97 Programs for Crystal Structure Solution and Refinement*, University of Gottingen, Gottingen, Germany, 1997.